FAIMS and phosphoproteomics of fibroblast growth factor signalling: Enhanced identification of multiply-phosphorylated peptides

Zhao, Hongyan; Cunningham, Debbie; Creese, Andrew; Heath, John; Cooper, Helen

[Link to publication on Research at Birmingham portal](#)

FAIMS and Phosphoproteomics of Fibroblast Growth Factor Signaling: Enhanced Identification of Multiply Phosphorylated Peptides

Hongyan Zhao, Debbie L. Cunningham, Andrew J. Creese, John K. Heath, and Helen J. Cooper*

School of Biosciences, University of Birmingham, Edgbaston, Birmingham B15 2TT, United Kingdom

S *Supporting Information*

ABSTRACT: We have applied liquid chromatography high-field asymmetric waveform ion mobility spectrometry tandem mass spectrometry (LC−FAIMS−MS/MS) and liquid chromatography tandem mass spectrometry (LC−MS/MS) to the investigation of site-specific phosphorylation in fibroblast growth factor (FGF) signaling. We have combined a SILAC approach with chemical inhibition by SU5402 (an FGF receptor tyrosine kinase inhibitor) and dasatinib (a Src family kinase inhibitor). The results show that incorporation of FAIMS within the workflow results in (a) an increase in the relative proportion of phosphothreonine and phosphotyrosine sites identified, (b) an increase in phosphopeptide identifications from precursors with charge states ≥ +3 (with an associated increase in peptide length), and (c) an increase in the identification of multiply phosphorylated peptides. Approximately 20% of the phosphorylation sites identified via the FAIMS workflow had not been reported previously, and over 80% of those were from multiply phosphorylated peptides. Moreover, FAIMS provided access to a distinct set of phosphorylation sites regulated in response to SU5402 and dasatinib. The enhanced identification of multiply phosphorylated peptides was particularly striking in the case of sites regulated by SU5402. In addition to providing a compelling example of the complementarity of FAIMS in phosphoproteomics, the results provide a valuable resource of phosphorylation sites for further investigation of FGF signaling and trafficking.

KEYWORDS: *FAIMS, differential ion mobility, FGF signaling, phosphoenrichment, phosphopeptides, phosphoproteomics*
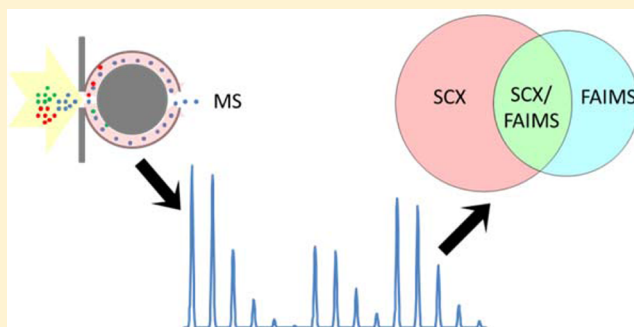
INTRODUCTION

Fibroblast growth factor (FGF) ligands and receptors play significant roles in cell division, regulation of cell growth and maturation, angiogenesis, wound healing, and tumor growth.[1] Accumulating evidence suggests that deregulation of FGF signaling is associated with many human diseases, including cancer.[2] Through phosphorylation and dephosphorylation processes, FGF signaling is propagated through receptor proteins, scaffolding proteins, and signal mediators, leading to a number of downstream pathways.[3] Of particular interest, the nonreceptor tyrosine kinase Src has been demonstrated to play a critical role in downstream FGFR trafficking.[4]

Considering their broad participation in signal transduction, it is not surprising that phosphorylation events hold the key to understanding signaling events downstream of FGFR. Improving proteome coverage is essential for mapping sites of phosphorylation. Functional interpretation of phosphorylation requires detailed analysis of specific residues or combinations of residues. For instance, phosphorylation of the active sites of kinases often significantly alters the binding capacity for substrates with consensus phosphorylation motifs.[5] The interaction between the docking motif on the substrate and the kinase regulates the specificity at the next level. In some cases, the recruitment of substrate to kinase requires phosphorylation of an adjacent or distant residue from the active site loop.[6]

For tryptic peptides, singly modified peptides constitute the majority of the total phosphopeptides identified by current technologies.[7] Current understanding suggests that it is more challenging to detect doubly and multiply phosphorylated peptides than singly phosphorylated peptides due to their low stoichiometry, ion suppression, and poor binding ability to chromatographic columns. Nevertheless, deciphering the mechanisms of FGFR signaling requires knowledge of multiply phosphorylated peptides, as these adjacent phosphorylation sites may play important regulatory roles. Therefore, one of the major challenges in intracellular cell signaling research is to map sites of modification in multiply phosphorylated peptides.

Liquid chromatography tandem mass spectrometry (LC−MS/MS) combined with prefractionation and phosphoenrichment is well-established as an effective workflow for large-scale quantitative phosphoproteomic analysis.[8] Although progress in this area has been made, low phosphoproteome coverage, limited dynamic range, and coelution of peptide isomers still remain

challenges. Researchers have endeavored to address these limitations through optimized phosphopeptide enrichment protocols,[9] liquid chromatography,[10] combinations of MS/MS approaches,[11] and development of novel data handling software.[12]

In recent years, ion mobility spectrometry (IMS) has emerged as an attractive technique for global proteome profiling. In field asymmetric waveform ion mobility spectrometry (FAIMS),[13] gas-phase ions are separated on the basis of differences in their mobility in high and low electric fields. In a FAIMS device, ions are introduced between planar or cylindrical electrodes, where they are exposed to alternating high and low electric fields. As a result of their differential ion mobilities, the ions will drift toward one or the other of the electrodes. By superimposing a dc compensation voltage (CV) to one of the electrodes, ions of particular differential ion mobility will be selectively transmitted through the device. Coupled with LC−MS/MS, FAIMS has been shown to be advantageous for proteomic analyses by improving signal-to-noise, extending proteome coverage, and separating isomeric peptides.[14−16] Bridon et al. described a 49% increase in phosphopeptide identification compared to that with conventional LC−MS/MS analysis.[17] They also evaluated the potential of FAIMS to enhance separation of isobaric phosphopeptides with 78 phosphopeptide isomers identified via FAIMS. Creese and co-workers compared workflows comprising prefractionation by strong cation exchange (SCX) chromatography and online reversed-phase LC−MS/MS with online reversed-phase LC−FAIMS−MS/MS for identification of peptides from whole cell lysates.[18] The results showed that inclusion of FAIMS extended the proteome coverage by 66.7%, highlighting the complementarity of FAIMS. Xia et al.[19] applied FAIMS in quantitative analysis toward the development of an LC−FAIMS−SRM method for quantitation of multiple analytes. They demonstrated that LC−FAIMS−SRM outperforms LC−SRM in terms of sensitivity and selectivity. Swearingen et al.[15] described the modification of the electrospray probe, together with the use of sheath gas to assist electrospray, which resulted in a 5-fold increase in the signal and 64% more protein identifications for LC−FAIMS−MS/MS over LC−MS/MS without FAIMS.

Here, we have applied LC−FAIMS−MS/MS to the investigation of site-specific phosphorylation in FGFR signaling. Previously, we have used quantitative LC−MS/MS to identify Src family kinase-mediated phosphorylation events in FGFR signaling.[20] To further map the key phosphorylation events involved in FGF signaling and its downstream Src family kinases (SFK), we used a stable isotope labeling with amino acids in cell culture (SILAC)[21] approach combined with inhibition of FGFR and SFK. SU5402,[22] a specific FGFR tyrosine kinase inhibitor, and dasatinib,[23] a SFK inhibitor, were used. The combination of chemical inhibition of the activities of FGFR and SFK enabled us to systematically investigate the participation of phosphosites in FGF signaling and allowed us to compare and evaluate the performance of LC−MS/MS and LC−FAIMS−MS/MS for phosphoproteomics more broadly.

■ MATERIALS AND METHODS

SUM52 Cell Culture

For SILAC labeling, SUM52 breast cancer carcinoma cells were cultured in amino acid-deficient RPMI-1640 (Thermo Fisher Scientific, Rockford, IL) containing either 0.274 mM isotopically "light" L-lysine and 1.15 mM L-arginine (Sigma-Aldrich, St. Louis,

MO), "medium" 4,4,5,5-D_4 L-lysine and $^{13}C_6$ L-arginine, or "heavy" $^{13}C_6$ L-lysine and $^{13}C_6$ $^{15}N_4$ L-arginine (Goss Scientific, Crewe, UK), supplemented with 10% dialyzed FBS (Thermo Fisher Scientific), 0.1 mg/mL streptomycin, and 100 IU/mL penicillin at 37 °C with 5% CO_2. The cells were cultured in medium for more than six population doublings to attain complete labeling.

Cell Treatment and Cell Lysis

After 4 h of serum starvation, "light" cells were treated with 20 ng/mL FGF1 and 10 mg/mL heparin for 30 min, "medium" cells were pretreated with 20 μM SU5402 for 30 min followed by treatment with 20 ng/mL FGF1 and 10 mg/mL heparin for 30 min, and "heavy" cells were pretreated with 1 μM dasatinib for 30 min followed by treatment with 20 ng/mL FGF1 and 10 mg/mL heparin for 30 min.

Prior to lysis, cells were washed twice in cold PBS and then lysed at 4 °C for 30 min in 800 μL of lysis buffer (50 mM Tris-HCl pH 7.4, 1% Triton TX-100, 150 mM NaCl, 1 tablet of protease inhibitor cocktail (Roche, Indianapolis, IN), and 1 tablet of phosphatase inhibitor cocktail (Roche, Indianapolis, IN) per 10 mL of buffer). Protein concentration of the resulting whole cell lysates was determined using the Coomassie (Bradford) protein assay kit (Thermo Fisher Scientific) according to the manufacturers' instructions.

Trypsin Digestion and Fractionation

A total of 30 mg of protein was used in the analysis. Ten milligrams of "light" (control), "medium" (SU5402 treated), and "heavy" (dasatinib treated) lysates was pooled prior to trypsin digestion. Proteins were reduced with 8 mM DTT, alkylated with 20 mM iodoacetamide in 50 mM ammonium bicarbonate, and finally digested with trypsin at a 1:100 enzyme/protein ratio (Promega, Madison, WI) at 37 °C overnight. The digestion was stopped by addition of 0.5% TFA. Prior to fractionation, peptides were desalted using Sep-Pak C18 Cartridge (Waters, Milford, MA) according to the manufacturer's instructions.

Desalted and dried peptides were resuspended in 100 μL of mobile phase A (10 mM KH_3PO_4, 20% acetonitrile, pH 3) and loaded onto a 100 × 4.6 mm polysulfethyl A column (5 μm particle size, 200 nm pore size, PolyLC, Columbia, MD). Peptides were separated with 0−50% mobile phase B (10 mM KH_3PO_4, 20% acetonitrile, 500 mM KCl, pH 3) over a 30 min gradient, which was increased to 100% B over 5 min. Fifty three fractions were collected. The fractions were combined into 12 fractions. Fractions were combined as follows: (1) 4 and 5, (2) 6, (3) 7, (4) 8, (5) 9 and 10, (6) 11, (7) 12 and 13, (8) 14−16, (9) 17−21, (10) 22−28, (11) 29−38, and (12) 39−53. Each of the 12 fractions was desalted using C8 cartridge (Michrom BioResources, Auburn, CA) according to the manufacturer's instructions.

Peptides in each of the 12 desalted fractions were divided in half. One half was enriched by used of Titansphere Phos-TiO kit (GL Sciences, Tokyo, Japan) according to the manufacturer's instructions. The other half was enriched using Titansphere Phos-TiO tips but using 1 M citric acid instead of lactic acid according to Zhao et al.[24] (Previous work in our laboratory showed that citric acid-assisted enrichment results in a 20% increase in the identification of multiply phosphorylated peptides (data not shown)). The half-fractions enriched via the two methods were recombined to give 12 enriched fractions. Each of the 12 fractions was desalted by use of C_{18} Ziptip pipette tips (Millipore, Billerica, MA) according to the manufacturers' instructions.

Each of the 12 fractions was subsequently split into two. One half of each of the fractions was destined for LC−MS/MS analyses. For the LC−FAIMS−MS/MS analyses, the remaining 12 half-fractions were pooled and divided equally into 12 aliquots to ensure that all FAIMS analyses were performed on the same peptide mixture. Each of these 12 aliquots was then analyzed at a separate compensation voltage (from −22.5 to −50 V in 2.5 V steps). Each of the 24 samples (12 half-fractions for LC−MS/MS and 12 aliquots for LC−FAIMS MS/MS) was split into four to allow two CID MS/MS analyses and, separately, two ETD MS/MS analyses. A schematic diagram of the sample preparation procedure is shown in Supporting Information Figure S1.

LC−MS/MS

Experiments were performed on a Thermo Fisher Orbitrap Velos ETD mass spectrometer (Thermo Fisher Scientific, San Jose, CA) equipped with a Dionex-Ultimate 3000 Nano LC system (Thermo Fisher Scientific, Sunnyvale, CA). Samples were loaded onto a 150 mm Acclaim PepMap100 C_{18} column (Thermo Fisher Scientific, Sunnyvale, CA), internal diameter 75 μm, in mobile phase A (0.1% formic acid) and separated by a 30 min gradient from 3.2 to 44% mobile phase B (acetonitrile, 0.1% formic acid), followed by a 10 min wash of 90% mobile phase B and re-equilibration (15 min) with 3.2% mobile phase B. Peptides were eluted via a TriVersa Nanomate (Advion, Ithaca, NY) chip-based electrospray device into the mass spectrometer. For both CID and ETD analyses, the mass spectrometer performed a top-seven method comprising a full FT−MS scan (m/z 380−1600) at a resolution of 30 000 at m/z 400 in the orbitrap with an automatic gain control (AGC) target of 1×10^6 charges and a maximum fill time of 1 s. The seven most abundant precursor ions detected were isolated for MS/MS in the ion trap. For CID, MS/MS of the seven most abundant ions above a threshold of 1000 with a normalized collision energy of 35% was performed (AGC target: 5×10^4 charges, maximum fill time 100 ms). For ETD, MS/MS of the seven most abundant ions above a threshold of 5000 with 100 ms activation time was performed (AGC target: 5×10^4 charges, maximum fill time 100 ms, reagent AGC target 1×10^5). Width of the precursor isolation window was 2 m/z, and only multiply charged precursor ions were subjected to fragmentation. Dynamic exclusion was applied for 60 s.

LC−FAIMS−MS/MS

The FAIMS device with a 2.5 mm electrode gap width (Thermo Fisher Scientific) was operated under the following conditions: gas flow rate of 2.9 L/min with a composition of 50:50 He/N_2, the dispersion voltage (DV) was −5000 V, and the inner and outer electrodes temperatures were 70 and 90 °C, respectively. Liquid chromatography was as described above. To couple nanospray, the HESI-II (Thermo Fisher Scientific) source was modified to accommodate a 360 μm o.d. fused silica capillary, with the addition of sheath gas (2 arbitrary units) for electrospray ionization, similar to that described by Swearingen et al.[15] Twelve separate LC−FAIMS−MS/MS analyses were performed at compensation voltages (CV) of −22.5, −25.0, −27.5, −30.0, −32.5, −35.0, −37.5, −40.0−42.5, −45.0, −47.5, and −50.0 V. MS/MS methods were as described above.

Identification and Quantitation of Peptide and Proteins

Mass spectra were processed using the MaxQuant software (version 1.4.1.3).[12] Data were searched against the SwissProt human database (downloaded in 2013) containing common contaminants and reverse sequence (175 242 protein entries).

The search parameters were as follows: minimum peptide length, 6; peptide tolerance, 20 ppm; mass tolerance, 0.5 Da; cleavage enzyme, trypsin/P; and 2 missed cleavages were allowed. Carbamidomethyl (C) was set as a fixed modification. Oxidation (M), acetylation (Protein N-term), and phospho (STY) were set as variable modifications. The appropriate SILAC labels were selected, and the maximum labeled amino acids was set to 3. False discovery rate (FDR) for peptide, protein, and site identification was set to 0.01. Within the Maxquant output, phosphorylation sites with a Localization Score above 0.75 were considered to be localized correctly, and the correctly localized phosphopeptides were selected for further analysis. Annotated MS/MS spectra for identified phosphopeptides are shown in Supporting Information Files 1A and 1B.

For quantitation analysis, SILAC ratios were normalized to avoid unimodal global distribution of peptide abundance. Normalization is automatically performed within the Maxquant software such that the median of the $\log_2$ peptide ratios is zero. This is performed for each data file analyzed.[12] A difference of a 2-fold change in SILAC ratio ($\log_2 \leq -1$ or $\log_2 \geq 1$) was considered to indicate a statistically significant change of lower or higher expression. The fold change cutoff value was applied based on data from a previous experiment performed in our laboratory (data not shown). In that experiment, samples labeled with light, medium, and heavy isotope labels were mixed in equal portions, (i.e., ratio = 1) and subjected to LC−MS/MS analysis. The mean SILAC ratio and standard deviation (SD) were calculated. For a probability cutoff of $p = 0.05$, the mean ratio $\pm$2SD was between 0.58 and 1.73. For a more stringent cutoff ($p = 0.0027$), the mean ratio $\pm$3SD was between 0.44 and 2.23. We therefore define the $|\log_2(FC)| = 1$ as the boundary of differentially regulated peptides to give greater than 95% confidence.

■ RESULTS AND DISCUSSION

Phosphopeptide Identification by LC−MS/MS and LC−FAIMS−MS/MS

When compared to conventional LC−MS/MS, LC−FAIMS−MS/MS has the advantage of enhancing signal-to-noise, thereby facilitating the identification of low-abundance ions.[17] In addition, FAIMS can separate peptide isomers and positional variants of post-translational modifications that may coelute in the absence of FAIMS.[16] These properties make FAIMS a valuable addition to phosphoproteomic studies, enhancing the coverage of the phosphoproteome and increasing the confidence of site localization. It has previously been shown that LC−MS/MS and LC−FAIMS−MS/MS are complementary in their coverage of the proteome,[18] and it is this complementarity that we wished to exploit in order to extend the phosphoproteomic coverage of components of the FGF signaling pathway.

We used a SILAC-based phosphoproteomic approach to compare phosphorylation events downstream of FGFR and Src family kinases in SUM52 cells. SILAC-labeled SUM52 cells (light, medium, and heavy) were treated with either SU5402 (FGFR inhibitor) or dasatinib (SFK inhibitor) before FGF1 stimulation. Following cell lysis, equal amounts of SILAC cells were pooled and digested with trypsin. Next, peptides were fractionated using SCX and enriched for phosphopeptides, and each of the resulting 12 fractions was then divided into two for separate LC−MS/MS and LC−FAIMS−MS/MS analyses. Prior to LC−FAIMS−MS/MS analysis, the 12 fractions were pooled before dividing them into 12 equal fractions to ensure

homogeneity while allowing a direct comparison to be made to the SCX-fractionated LC—MS/MS samples in terms of sample preparation. Each LC—FAIMS—MS/MS analysis was performed at a separate and constant compensation voltage (−22.5, −25.0, −27.5, ..., −50.0 V, in 2.5 V steps). The CV range was chosen based on previous experiments in our laboratory using the range −20 to −55 V, which showed that 94.3% of the total number of identified phosphopeptides came from the CV range −22.5 to −50 V. In selecting a CV range, it is important to consider the balance between the number of CV steps (i.e., individual analyses) required and the number of fractions into which the sample can be split. All samples were analyzed in duplicate. This approach allowed us to directly compare the performance of LC—MS/MS and LC—FAIMS—MS/MS and examine their potential for characterization of phosphopeptides.

In total, 2538 well-localized phosphorylation sites were identified (1% false discovery rate) using MaxQuant.[12] In LC—MS/MS analyses, a total of 3197 nonredundant peptides were identified, of which 2741 were phosphopeptides (85.7%). Within these phosphopeptides, there are a total of 2642 phosphosites, of which 1853 (70.1%) phosphosites were accurately localized (Supporting Information Table S1A). The distribution of phosphorylated residues is 1542 serine (83.2%), 207 threonine (11.1%), and 104 tyrosine (5.6%). Around 40% of the unique identifications in the FAIMS data set derived from peptides containing sites of missed tryptic cleavages, compared to 27% in the non-FAIMS data set. In the LC—FAIMS—MS/MS analyses, a total of 1774 nonredundant peptides were identified, of which 1529 were phosphopeptides (86.2%). From these phosphopeptides, 1930 phosphosites were identified and 1261 phosphosites were well-localized (65.2%) (Supporting Information Table S1B). Within the well-localized phosphosites, 897 (71.1%) serine, 264 (20.9%) threonine, and 100 (7.9%) tyrosine residues were identified. Notably, an increase in the relative proportion of identified pThr and pTyr phosphorylation sites was observed in the LC—FAIMS—MS/MS data set. It has been estimated that the distribution of pSer, pThr, and pTyr sites is expected to be around 86.4, 11.8, and 1.8%, respectively, in eukaryotic cells.[25] The successful identification of tyrosine phosphorylation is particularly challenging, as it is a substoichiometric modification often occurring on low-abundance proteins.[26] Moreover, knowledge of tyrosine phosphorylation is considered to be a key in deciphering the mechanisms of signal transduction processes and regulation of enzymatic activity. Therefore, the observation that pTyr sites are enriched in the FAIMS data set is particularly promising for phosphoproteomics in general.

In total, fewer phosphosites were identified from the LC—FAIMS—MS/MS data set than the LC—MS/MS data set. This observation is likely due to low transmission efficiency of FAIMS (∼10−20%). Nevertheless, the two approaches showed good complementarity, and the overlapping population comprised 44.0% of the identifications by LC—FAIMS—MS/MS (Figure 1A). In addition, samples analyzed by FAIMS were homogeneous, whereas samples analyzed by the non-FAIMS approach were fractioned by SCX chromatography (see Supporting Information Figure S1). This difference will contribute to variations in electrospray ionization efficiency, reversed-phase LC separation, and, consequently, MS/MS identification.

The scale of this experiment is not designed to reveal the whole map of FGF signaling and its downstream networks but to generate a complementary set of phosphosites that provides novel insights into the field of phosphoproteomic research. The stochastic nature of LC—MS/MS sampling can result in
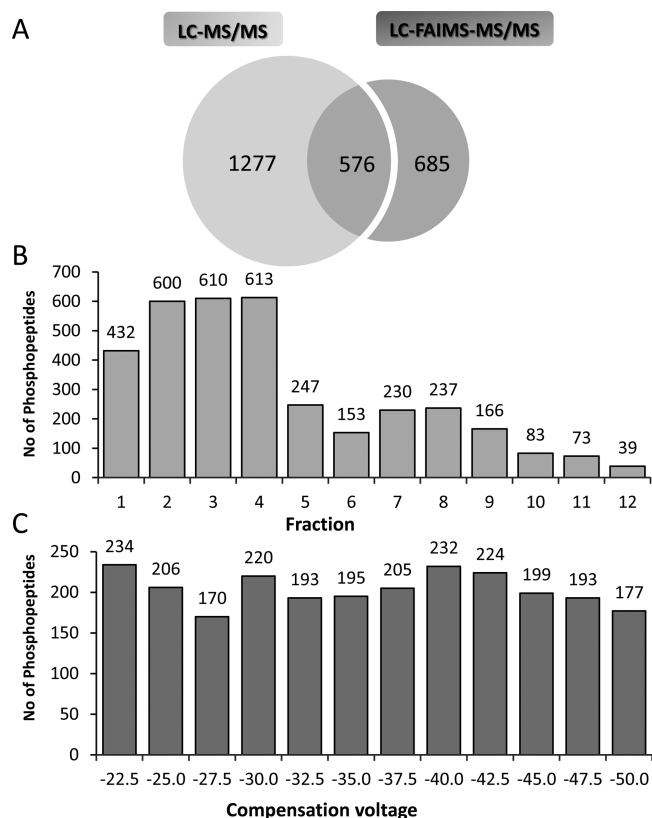
Figure 1. (A) Well-localized phosphorylation sites identified via LC—MS/MS and LC—FAIMS—MS/MS. (B) Distribution of phosphopeptides in LC—MS/MS analyses. (C) Distribution of phosphopeptides in LC—FAIMS—MS/MS analyses.

complementary peptide identifications in technical repeats; however, the application of FAIMS resulted in a distinct subset of phosphosites, which is evidenced by a 37.0% increase in phosphoproteome coverage. Note that a similar increase in phosphoproteome coverage was observed following multiple replicates ($n = 2$) of LC—MS/MS analyses (∼25% for CID and ∼40% for ETD; see Supporting Information Figure S2); however, the properties of the phosphopeptides identified by FAIMS are intrinsically different from those identified by LC—MS/MS, as described below. In order to investigate the properties of phosphopeptides identified in the LC—FAIMS—MS/MS workflow, we examined the CV distribution, charge state, length, and phosphorylation status of these phosphopeptides.

LC—FAIMS—MS/MS Identification of Phosphopeptides Is Not Biased toward CV

The number of nonredundant peptides identified per SCX fraction is shown in Figure 1B. In the LC—MS/MS analysis with SCX prefractionation, the majority of the peptides identified were from the first four SCX fractions (64.7%). In contrast, in the LC—FAIMS—MS/MS analyses (Figure 1C), phosphopeptide identification did not show any bias toward particular (range of) CV values. In the LC—FAIMS—MS/MS analysis, samples from all SCX fractions were pooled to ensure homogeneity while allowing a direct comparison to be made in terms of sample preparation. Therefore, the distribution of phosphopeptides is based solely on the transmission at preset CV values. In an acidic solution (e.g., pH 3), most tryptic peptides carry ≥2+ charges; however, many tryptic phosphopeptides carry 1+ or even
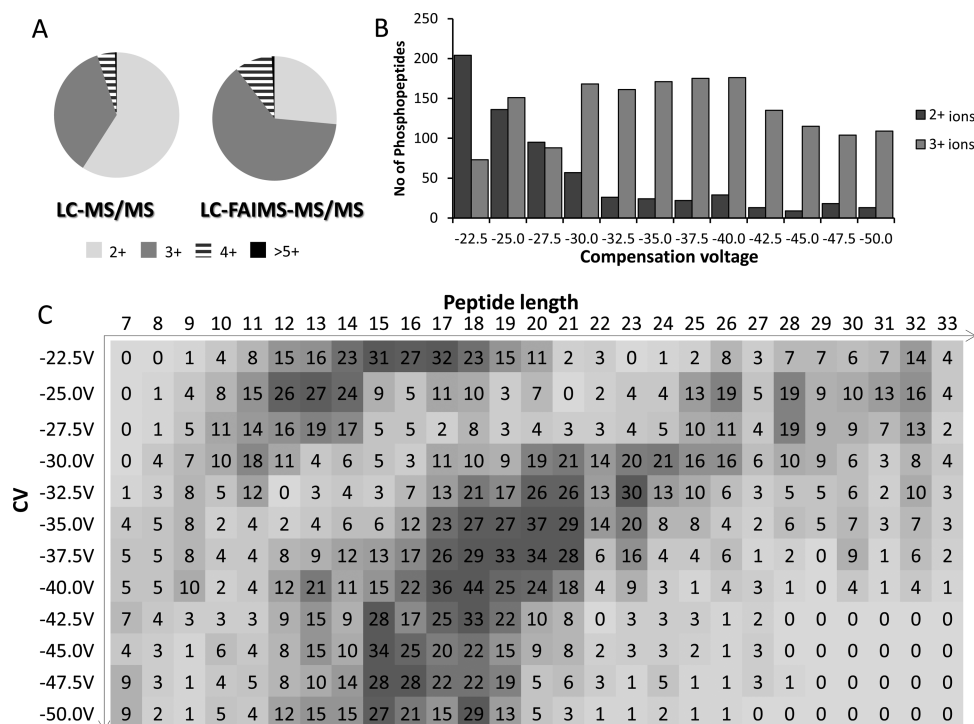
Figure 2. (A) Summary of phosphopeptides identifications according to charge state. (B) Distribution of identified phosphopeptides across CV values according to charge state. (C) Distribution of identified phosphopeptides according to CV and length (number of amino acid residues). Numbers in each cell represent the number of phosphopeptides identified under a given condition.

Figure 2C — Distribution of identified phosphopeptides according to CV and peptide length:

CV	7	8	9	10	11	12	13	14	15	16	17	18	19	20	21	22	23	24	25	26	27	28	29	30	31	32	33
-22.5V	0	0	1	4	8	15	16	23	31	27	32	23	15	11	2	3	0	1	2	8	3	7	7	6	7	14	4
-25.0V	0	1	4	8	15	26	27	24	9	5	11	10	3	7	0	2	4	4	13	19	5	19	9	10	13	16	4
-27.5V	0	1	5	11	14	16	19	17	5	5	2	8	3	4	3	3	4	5	10	11	4	19	9	9	7	13	2
-30.0V	0	4	7	10	18	11	4	6	5	3	11	10	9	19	21	14	20	21	16	16	6	10	9	6	3	8	4
-32.5V	1	3	8	5	12	0	3	4	3	7	13	21	17	26	26	13	30	13	10	6	3	5	5	6	2	10	3
-35.0V	4	5	8	2	4	2	4	6	6	12	23	27	27	37	29	14	20	8	8	4	2	6	5	7	3	7	3
-37.5V	5	5	8	4	4	8	9	12	13	17	26	29	33	34	28	6	16	4	4	6	1	2	0	9	1	6	2
-40.0V	5	5	10	2	4	12	21	11	15	22	36	44	25	24	18	4	9	3	1	4	3	1	0	4	1	4	1
-42.5V	7	4	3	3	3	9	15	9	28	17	25	33	22	10	8	0	3	3	3	1	2	0	0	0	0	0	0
-45.0V	4	3	1	6	4	8	15	10	34	25	20	22	15	9	8	2	3	3	2	1	3	0	0	0	0	0	0
-47.5V	9	3	1	4	5	8	10	14	28	28	22	22	19	5	6	3	1	5	1	1	3	1	0	0	0	0	0
-50.0V	9	2	1	5	4	12	15	15	27	21	15	29	13	5	3	1	1	2	1	1	0	0	0	0	0	0	0

negative charges due to the addition of phosphate groups.[27] In SCX chromatography, peptides are eluted according to their net charge states: multiply phosphorylated peptides are eluted first as the result of their negative charge, followed by singly phosphorylated peptides, missed cleavage phosphopeptides, and, finally, nonphosphopeptides. An enrichment of phospho-peptides was, therefore, observed in the first few fractions. This uneven distribution of phosphopeptides across the 12 LC−MS/MS fractions potentially lowers the efficiency of peptide identification, as evidenced by the under-representation of phosphopeptides in the latter eight SCX fractions (35.3% of the total identifications). The extent of proteome coverage is proportional to the degree of peptide fractionation and the resolving power of the mass spectrometer.

Triply Protonated Ions Are Enriched in LC−FAIMS−MS/MS

The distribution of identified phosphopeptides in terms of charge state is shown in Figure 2A. Doubly charged phosphopeptide ions (57.7%) constituted the majority of identifications from the LC−MS/MS data set, with triply charged ions contributing to 36.6% of the identifications. Further examination of these phosphopeptides revealed that the majority of the doubly charged peptides were identified from the first four fractions (see Supporting Information Figure S3A). The triply charged peptides show a bimodal distribution. These distribu-tions agree with the pH-dependent elution from SCX cartridges, where phosphopeptides are eluted first due to their negative charge, followed by nonphosphopeptides and then acidic peptides. For the LC−FAIMS−MS/MS data set, 26.9% of the total identifications arose from 2+ precursor ions, compared with 63.8% from 3+ ions. Further examination of the LC−FAIMS−MS/MS data set revealed that the 2+, 3+, and 4+ charged peptides were identified at distinctly different CV ranges (Figure 2B), which has been previously observed.[28] Doubly charged

phosphopeptide ions were observed mainly in the CV range −22.5 to −30.0 V (72.8%); however, 3+ and 4+ (data not shown) phosphopeptide ions were identified throughout all CVs.

One of the difficulties in phosphopeptide detection is low protonation efficiency in the presence of acidic phosphate groups. Doubly charged species are normally the predominant ions observed following electrospray of tryptic peptides. By coupling FAIMS to LC−MS/MS, an enrichment of 3+ and 4+ phosphopeptide ions was observed within the CV range −22.5 to −30.0 V. The results suggest that the charge-based selection afforded by the FAIMS device influences the phosphopeptides identified.

Phosphopeptide Length

The length of the phosphopeptides identified in the FAIMS data set ranged from 7 to 40 amino acids, 98.6% of which were between 7 and 33 amino acids. The phosphopeptide distribution according to CV and peptide length (7−33 amino acids) is shown in Figure 2C (the number in each cell represents the number of phosphopeptides identified). The heat map identified two areas with high incidence of phosphopeptide identification. One was in the CV range −22.5 to −27.5 V and length 12−18 amino acids. The other area was in the CV range −32.5 to −47.5 V and length 15−21 amino acids. These two regions overlap with the charge state distribution discussed above. For peptides identified from LC−MS/MS analyses, 64.7% peptides were identified from the first four fractions and the majority of the peptides were between 11 and 23 amino acid residues in length (see Supporting Information Figure S3).

Enhanced Identification of Multiply Phosphorylated Peptides

The distribution of singly, doubly, and multiply phosphorylated peptides is shown in Figure 3A,B. The majority of the phosphopeptide assignments were singly phosphorylated in

Multiply-phosphorylated peptides
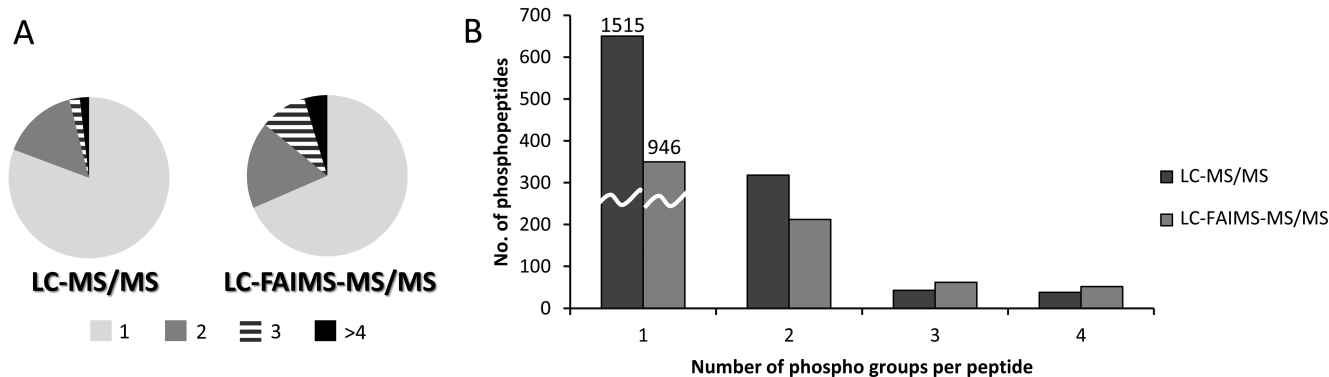
Figure 3. (A) Distribution of singly, doubly, multiply phosphorylated peptides. (B) Bar chart comparison of singly, doubly, multiply phosphorylated peptides in FAIMS and non-FAIMS analyses.
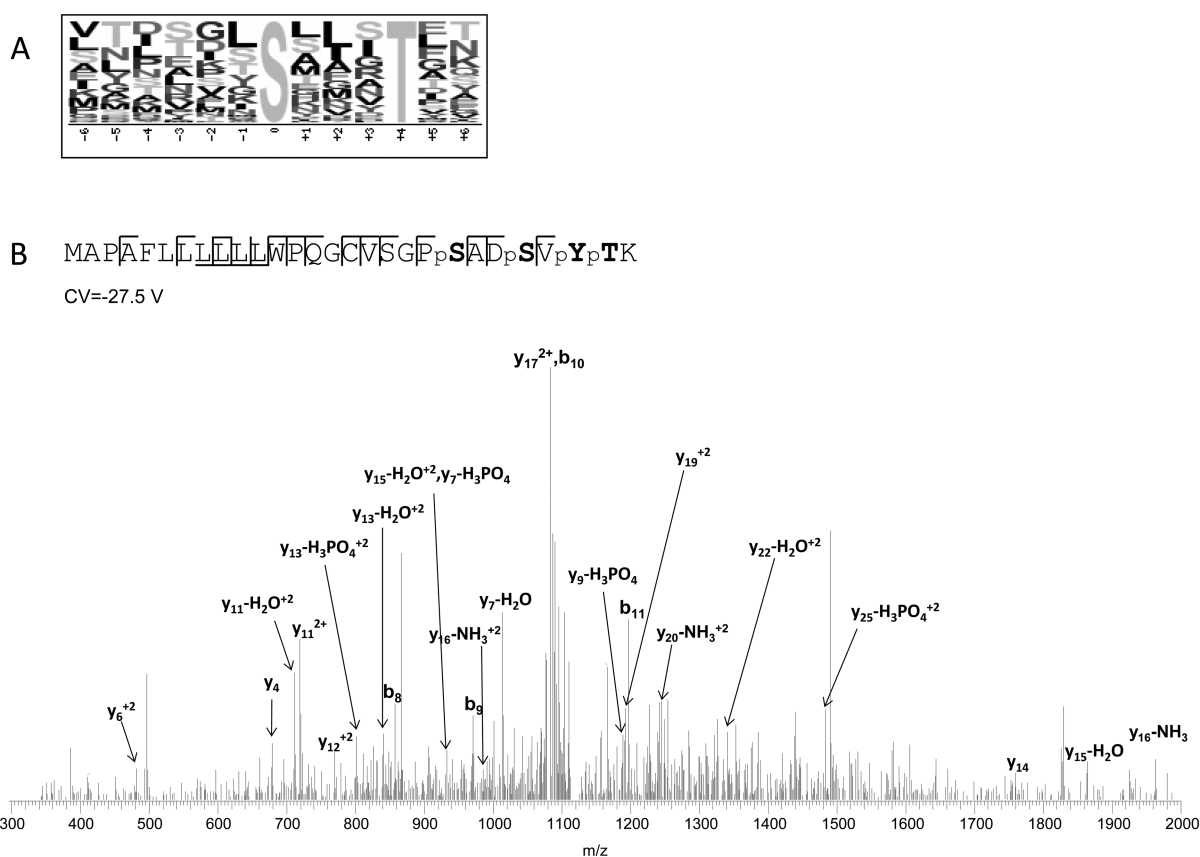

Figure 4. (A) Results from Motif-X analysis of the novel phosphorylation sites identified via LC−FAIMS−MS/MS showing motif SxxxT. (B) CID mass spectrum of $[M + 3H]^{3+}$ ions of MAPAFLLLLLLWPQGCVSGPpSADpSVpYpTK at a CV of −27.5 V, a multiply phosphorylated peptide containing previously unobserved sites of phosphorylation.

both methods (70.5% in LC−FAIMS−MS/MS analyses and 80.7% in LC−MS/MS analyses). A total of 29.5% of the phosphopeptides identified by the LC−FAIMS−MS/MS workflow were doubly or multiply phosphorylated peptides, compared with 19.3% by the LC−MS/MS workflow.

The enhanced detection of multiply phosphorylated peptides is significant in view of their low abundance relative to that of singly and nonphosphorylated peptides. Generally, it is more challenging to detect multiply phosphorylated peptides due to their low ionization efficiency in the electrospray process and their poor binding ability to chromatographic columns. This observation may be the result of the improved signal-to-noise

afforded by FAIMS or charge state differentiation via FAIMS as discussed above. The identification of singly and multiply phosphorylated peptides did not show any correlation with the distribution of CV. The distribution of charge states for the multiply phosphorylated peptides identified is shown in Supporting Information Figure S4. The multiply phosphorylated peptides are associated with 3+ and higher charge states in the FAIMS data set compared to non-FAIMS. The enhanced identification of multiply phosphorylated peptides is likely due to the separation of charge states by FAIMS.

Successful identification of multiply phosphorylated peptides and localization of the phosphorylation sites therein also has a
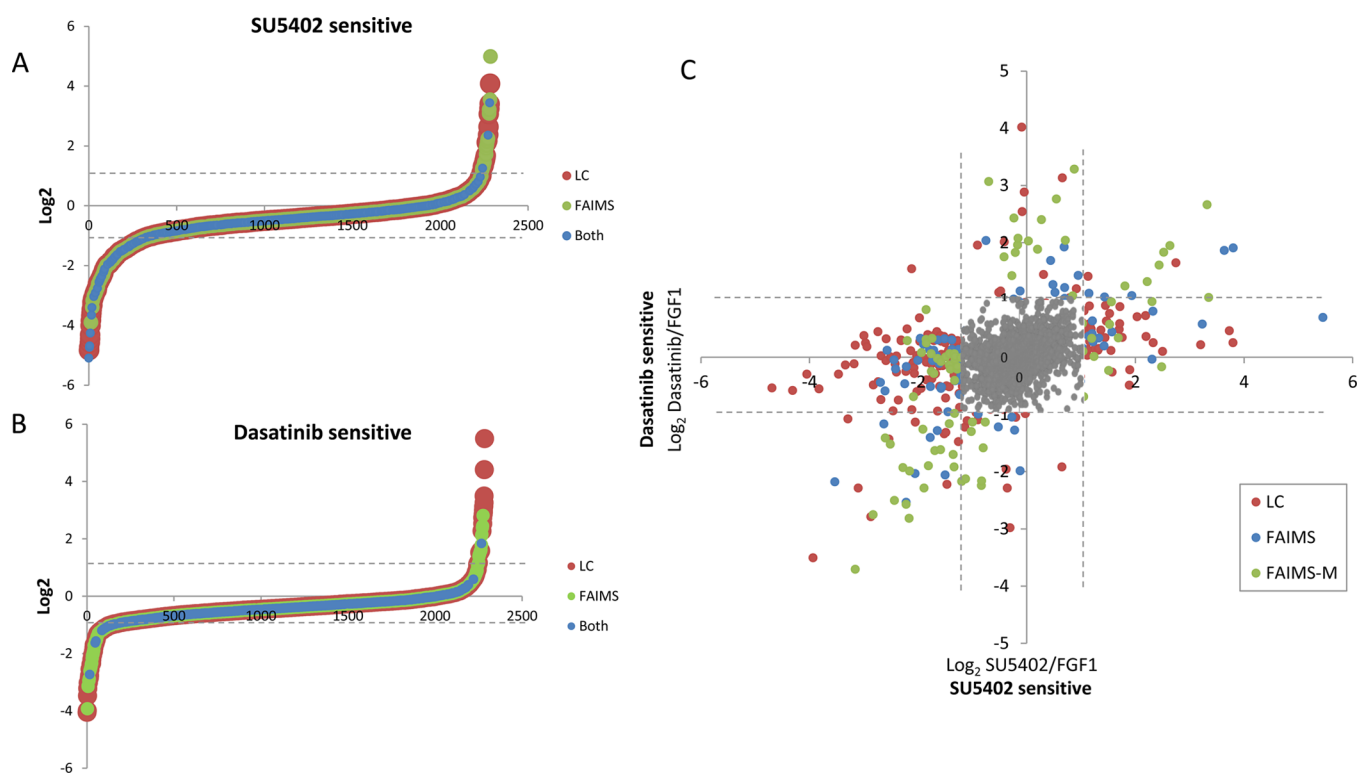
Figure 5. (A) Log$_2$ plot of the peptide abundance ratio for SU5402/FGF1 treatments for each phosphopeptide identified. (B) Log$_2$ plot of the ratio of the peptide abundance ratio for dasatinib/FGF1 treatments for each phosphopeptide identified. Peptides identified by FAIMS only are shown in green, and those identified by LC−MS/MS only are shown in red. Peptides identified by both are shown in blue. Dashed lines indicate the cutoff (log$_2$ = ±1). (C) Log$_2$−log$_2$ plots to visualize SU5402- and dasatinib-sensitive phosphopeptides. The peptide abundance ratio for SU5402/FGF1 treatments is plotted against the peptide abundance ratio for dasatinib/FGF1 treatments. Peptides identified by LC−MS/MS only are shown in red; singly phosphorylated and multiply phosphorylated peptides identified by FAIMS only are shown in blue and green, respectively. Those identified by both methods are shown in gray. Dashed lines indicate the cutoff (log$_2$ = ±1).

profound impact on data interpretation, enabling one to evaluate the coordination between two or more adjacent phosphorylation sites or to investigate the dynamics between singly and multiply phosphorylated peptide forms. In Supporting Information Figure S5, we show that the overlap in doubly phosphorylated peptide identifications from the two techniques was 21.2%. For multiply phosphorylated peptides (>2 phosphosites), only 7 of the 188 phosphopeptides were identified by both methods, less than 4% of the total multiply phosphorylated peptide identifications, emphasizing the complementarity of the two methods for identification of phosphopeptides, particularly multiply phosphorylated peptides.

Novel Phosphorylation Sites

To further probe the two data sets, PhosphoSitePlus (http://www.phosphosite.org)[29] was used to distinguish novel phosphorylation sites from known sites. In the LC−MS/MS workflow, 75 (4.3%) identified phosphosites were novel phosphorylation sites consisting of 33 pSer, 9 pThr, and 33 pTyr sites (Supporting Information Table 1A, shown in green). Only three of these sites were also identified in the LC−FAIMS−MS/MS data set. In contrast, a substantial number of phosphosites (19.9%) identified by LC−FAIMS−MS/MS workflow have not been previously reported (Supporting Information Table S1B, shown in green). A total of 227 novel phosphorylation sites were identified, consisting of 168 pSer, 42 pThr, and 17 pTyr. In total, 127 proteins were successfully assigned from these novel sites. Remarkably, 187 of the novel phosphorylation sites were identified within multiply phosphory-

lated peptides. Again, this observation highlights the advantages of FAIMS in identification of multiply phosphorylated peptides. These results show that coupling FAIMS to an LC−MS/MS platform in phosphoproteomic analyses not only extends the proteome coverage but also generates a large set of uncharacterized phosphorylation sites, suggesting that FAIMS has specifically accessed a group of phosphosites not readily accessible by LC−MS/MS.

In order to explore the sequence features of the novel sites, Motif-X[30] was used to identify motifs within the novel phosphorylation sites in the LC−FAIMS−MS/MS data set. From 227 phosphorylation sites, 3 potential motifs were identified (*P* < 0.0003): SxxT, SxxxT, and TxxxxS. The motif SxxxT is highly conserved and recognized by the MAPKK supergene family in animals (Figure 4A).[31] As promotion and attenuation of FGF signaling requires the involvement of the MAPKK cascade, this observation indicates that these substrates of MAPKK with uncharacterized phosphorylation sites may possess interesting properties for further investigation. No consensus motif was found following a similar analysis of the novel phosphorylation sites identified from the LC−MS/MS data set.

To determine if the enhancement in novel phosphorylation site identification was associated with charge state, we profiled the charge state distribution of the novel phosphorylation sites. In the LC−FAIMS−MS/MS analyses, phosphopeptides with charge states ≥3+ represented 91.2% of the novel sites identified, compared to 55.3% in LC−MS/MS analyses. Again, the overrepresentation of 3+ charged ions in LC−FAIMS−MS/

MS data set may be responsible for the increase in the number of novel sites.

Further analysis by DAVID functional classification[32] revealed that a cluster of G protein-coupled receptors (GPCRs) was enriched in the novel proteins identified in the LC−FAIMS−MS/MS workflow. An example of this is Trem-like transcript 2 (TLT-2) protein, a cell surface receptor protein that may play a role in immune response.[33] A quadruply phosphorylated peptide MAPAFLLLLLLWPQGCVSGPpSADpSVpYpTK of TLT-2 including the signal peptide region (1−18) was identified at a CV of −27.5 V (Figure 4B). The signal peptide region is not phosphorylated, but the N-terminus of Ig-like V-set domain (19−268) is highly phosphorylated, and this is the first time that phosphorylation sites have been reported within this region. This peptide was found to be downregulated in response to SU5402 treatment but not sensitive to dasatinib. Whether these phosphorylation sites on the N-terminus are involved in cleavage of signal peptides or signal recognition is yet unknown. An in-depth analysis is required to establish the cross-talk between these phosphorylation events and perturbation of FGF signaling.

Identification of FGFR and Src-Mediated Phosphorylation Events

The LC−FAIMS−MS/MS workflow enabled a distinct phosphopeptide data set to be identified. In order to map the novel phosphopeptides regulated in response to SU5402 and dasatinib, a wide-scale quantitative analysis was performed. A comparative analysis of phosphosites sensitive to SU5402 identified by LC−MS/MS only, by LC−FAIMS−MS/MS only, and by both is shown in Figure 5A. The consistency of the two approaches is shown in Supporting Information Figure S6. A high occurrence of global downregulation in phosphorylation levels involved in the FGF pathway and downstream processes was observed. A total of 256 phosphosites sensitive to SU5402 ($\log_2 \leq -1$ or $\log_2 \geq 1$) were detected by both methods (Figure 5A, shown in blue). LC−MS/MS and LC−FAIMS−MS/MS resulted in identification of 175 phosphosites (shown in red) and 153 phosphosites (shown in green) sensitive to SU5402 treatment (Supporting Information Table S1A,B). A total of 186 phosphosites were downregulated as a result of SU5402 treatment, of which 70 were uniquely identified via the FAIMS workflow. Seventy four phosphosites were found to be upregulated in response to SU5402, with 29 of them being unique to the FAIMS workflow. Two clusters of proteins were enriched from the regulated peptides in response to SU5402. One is a group of kinases involved in cell cycle regulation and translation. For example, Ribosomal protein S6 kinase beta-2 (RPS6KB2, also known as S6K2) with decreased phosphorylation upon SU5402 and dasatinib inhibition was identified in FAIMS analysis. S6K2 has been previously identified as a downstream effector of FGF signaling.[34] The other cluster contains a group of cell membrane receptors that participate in signal transduction and transportation, including LILRB1 and MRG.

A total of 87 phosphosites sensitive to dasatinib treatment were detected by both methods (Figure 5B). LC−MS/MS and LC−FAIMS−MS/MS resulted in identification of 24 and 60 phosphosites sensitive to dasatinib treatment, respectively. A total of 40 phosphosites were downregulated as a result of dasatinib treatment, of which 27 were uniquely identified via the FAIMS workflow. Forty seven phosphosites were found to be upregulated in response to dasatinib, with 32 of them being unique to the FAIMS workflow.

The LC−MS/MS and LC−FAIMS−MS/MS data sets were further investigated to interrogate the coordination between SU5402 and dasatinib. A log−log plot was used to visualize the underlying interaction (Figure 5C). A total of 53 phosphosites sensitive to both SU5402 and dasatinib treatment were identified. LC−FAIMS−MS/MS alone revealed 38 phosphosites sensitive to both treatments, and 2 phosphopeptides were found by both approaches.

As described above, an enrichment of multiply phosphorylated peptides was observed in the peptides identified by LC−FAIMS−MS/MS: a total of 67 (55.8%) of the phosphosites sensitive to SU5402 were from multiply phosphorylated peptides, compared with 6 identified from the LC−MS/MS data set. Similarly, 46 out of 70 phosphosites sensitive to dasatinib originated from multiply phosphorylated peptides. Furthermore, among the 67 phosphosites identified as sensitive to SU5402, 31 were novel. The results, therefore, provide a useful starting point for follow-up functional investigations. A list of novel phosphorylation sites identified from multiply phosphorylated peptides sensitive to SU5402 or dasatinib treatment is presented in Supporting Information Table S2.

Overall, the results show that chemical inhibition induced significant changes in ∼17% of the measured phosphosites. Although some of the identified proteins were already known to be associated with FGF signaling, many of the individual proteins or phosphosites identified are novel to this pathway. As an example, breast cancer anti-estrogen resistance protein 3 (BCAR3) acts as an adapter protein for tyrosine kinase-based signaling in breast cancer cells.[35] The FAIMS results revealed a previously unidentified phosphorylation site within this protein: threonine 368 (T368). BCAR3 has been shown to enhance cell mobility through interaction with Src and p130^{cas}. It has been suggested that this binding capacity would be greatly reduced when Src activity is affected.[36] The phosphorylation level of T368 site was upregulated upon SU5402 and dasatinib treatment. Whether the upregulation of T368 is associated with the activity of BCAR3 is unknown: this result may provide a meaningful entry point to decipher mechanisms of estrogen regulation.

Our findings demonstrate that FAIMS offers superior performance to LC−MS/MS in the identification and characterization of peptides with multiply phosphorylated residues. It has been demonstrated, on both theoretical and experimental grounds, that multisite phosphorylation can generate a switch-like temporal profile of the response to a graded input[37] and, when executed in a specific sequence, that it can dictate the timing of output responses.[38,39] However, judged by existing phosphosite databases, the extent and identity of multisite phosphorylation events are poorly defined compared to that for single-site events. Current bioinformatic software focuses mainly on interpretation of single phosphosites rather than interaction of multiphosphorylation sites, e.g., iGPS analysis of the data sets predicts which kinases are phosphorylating the peptides (Supporting Information Figure S7A).[40] It is clear that more of the peptides are predicted to be phosphorylated by known kinases in the non-FAIMS data set. Kinases with a variety of biological functions were identified, but, generally, FAIMS provides a small and complementary fraction. This is likely because in the FAIMS data set 29.5% of identified phosphorylation sites and 55.8% of phosphorylation sites sensitive to inhibitors were identified from multiply phosphorylation sites. The ability to efficiently define multisite phosphorylation events is of particular biological significance, as they represent a significant regulatory mechanism in a variety of settings. Analysis

of amino acid frequency in the phosphopeptide sequences (Supporting Information Figure S7B) was performed using Weblogo (http://weblogo.berkeley.edu/logo.cgi). We observed a higher frequency of serine residues in proximity to the site of phosphorylation in the FAIMS data set compared to that in the non-FAIMS data set because of the multiply phosphorylated peptides.

In particular, phosphorylation of tyrosine residues is a well-defined mechanism of eliciting protein/protein interaction via sequence-specific recognition by phosphotyrosine binding motifs such as SH2 domains.[40] Recognition of phosphotyrosine motifs can be modified by concurrent phosphorylation of adjacent Ser/Thr residues that occlude the SH2 binding pocket.[41] This results in a gated output where the formation/dissolution of protein complexes is controlled by the combined action of Tyr and Ser/Thr directed kinases. It is notable that inspection of the multiply phosphorylated phosphopeptides identified in the FAIMS data set (Supporting Information Table S1B, column H) reveals a significant fraction (58.4%) in which a phosphorylated tyrosine residue is located within ±4 residues of a phospho-Ser/Thr. This indicates that this class of multisite phosphorylation is a prevalent regulatory event that can be preferentially addressed by the application of FAIMS. Moreover, this points to the work that can be potentially carried out in the next step, which will focus on the dynamics of key phosphorylation sites within FGF signaling. The site-specific analysis of key phosphorylation sites, especially the interdependence among multiphosphorylation sites, will be of great interest to determine the downstream network of FGF perturbation.

CONCLUSIONS

Our LC−MS/MS and LC−FAIMS−MS/MS analyses combined SILAC labeling with SCX prefractionation and phosphoenrichment. This approach allowed us to investigate the regulated phosphorylation events involved in FGF signaling. The two techniques showed good complementarity. The application of FAIMS extends the phosphoproteome coverage by 37.0% over that identified with the conventional LC−MS/MS workflow. Although the number of phosphosites identifications by LC−FAIMS−MS/MS is lower in general, the improvement in the detection of pThr and pTyr sites provides a valuable pool for further analysis. An enhancement in the identification of multiply phosphorylated peptides and a preference for peptides with high charge states (3+ and above) were observed in the LC−FAIMS−MS/MS data set. We propose that this enhancement is closely associated with the charge-based selection of FAIMS. Although the scale of this experiment was not designed to reveal the whole map of FGF signaling, our results provide a unique resource of phosphosites for further study and a compelling example of the utility of FAIMS in phosphoproteomics research. This claim is evidenced by the observation that 20% of the phosphosites identified via by FAIMS have not been reported previously. Moreover, 82.3% of these novel sites are identified from multiply phosphorylated peptides. The LC−FAIMS−MS/MS workflow also revealed a substantial number of phosphopeptides regulated upon drug treatment, especially multiply phosphorylated peptides. Hence, we propose that the LC−FAIMS−MS/MS workflow is a suitable complementary approach in phosphoproteomic analysis. Together, these observations open new possibilities for in-depth characterization of interesting candidates for their roles in FGF signaling and trafficking.

ASSOCIATED CONTENT

Ⓢ Supporting Information

The Supporting Information is available free of charge on the ACS Publications website at DOI: 10.1021/acs.jproteome.5b00713.

Schematic diagram of the sample preparation procedure and MS/MS analyses (Figure S1); overlap between the duplicate analyses in LC−MS/MS and LC−FAIMS−MS/MS analyses (Figure S2); distribution of 2+ and 3+ phosphopeptides in the LC−MS/MS data set and distribution of identified phosphopeptides according to fraction no. and peptide length (number of amino acid residues) in the LC−MS/MS data set (Figure S3); distribution of charge states of multiply phosphorylated peptides (Figure S4); summary of multiply phosphorylated peptide identifications (Figure S5); histogram showing the quantitation consistency between LC−MS/MS and LC−FAIMS−MS/MS assays (Figure S6); heat map showing proteins and kinases predicted to phosphorylate substrates in FAIMS and non-FAIMS data sets and motif analysis of phosphorylation sites in FAIMS and non-FAIMS data sets (Figure S7) (PDF)

Phosphopeptide identifications with well-localized sites of modification (Table S1); novel phosphorylation sites sensitive to SU5402 and/or dasatinib identified within multiply phosphorylated peptides in the LC−FAIMS−MS/MS data set (Table S2) (XLSX)

Annotated MS/MS spectra of identified phosphopeptides (PDF, PDF)

AUTHOR INFORMATION

Corresponding Author

*E-mail: h.j.cooper@bham.ac.uk. Tel: +44 (0)121 414 7527.

Notes

The authors declare no competing financial interest.

ACKNOWLEDGMENTS

REFERENCES

(1) Wesche, J.; Haglund, K.; Haugsten, E. M. Fibroblast growth factors and their receptors in cancer. *Biochem. J.* **2011**, *437*, 199−213.

(2) Greenman, C.; Stephens, P.; Smith, R.; Dalgliesh, G. L.; Hunter, C.; Bignell, G.; Davies, H.; Teague, J.; Butler, A.; Stevens, C.; et al. Patterns of somatic mutation in human cancer genomes. *Nature* **2007**, *446*, 153−158.

(3) Tenhagen, M.; van Diest, P. J.; Ivanova, I. A.; van der Wall, E.; van der Groep, P. Fibroblast growth factor receptors in breast cancer: expression, downstream effects, and possible drug targets. *Endocr.-Relat. Cancer* **2012**, *19*, R115−R129.

(4) Sandilands, E.; Akbarzadeh, S.; Vecchione, A.; McEwan, D. G.; Frame, M. C.; Heath, J. K. Src kinase modulates the activation, transport

and signalling dynamics of fibroblast growth factor receptors. *EMBO Rep.* **2007**, *8*, 1162−1169.

(5) Ubersax, J. A.; Ferrell, J. E., Jr. Mechanisms of specificity in protein phosphorylation. *Nat. Rev. Mol. Cell Biol.* **2007**, *8*, 530−541.

(6) Pinna, L. A.; Ruzzene, M. How do protein kinases recognize their substrates? *Biochim. Biophys. Acta, Mol. Cell Res.* **1996**, *1314*, 191−225.

(7) Steen, H.; Jebanathirajah, J. A.; Rush, J.; Morrice, N.; Kirschner, M. W. Phosphorylation analysis by mass spectrometry: myths, facts, and the consequences for qualitative and quantitative measurements. *Mol. Cell. Proteomics* **2006**, *5*, 172−181.

(8) Mann, M.; Ong, S.-E.; Grønborg, M.; Steen, H.; Jensen, O. N.; Pandey, A. Analysis of protein phosphorylation using mass spectrometry: deciphering the phosphoproteome. *Trends Biotechnol.* **2002**, *20*, 261−268.

(9) Fukuda, I.; Hirabayashi-Ishioka, Y.; Sakikawa, I.; Ota, T.; Yokoyama, M.; Uchiumi, T.; Morita, A. Optimization of enrichment conditions on TiO2 chromatography using glycerol as an additive reagent for effective phosphoproteomic analysis. *J. Proteome Res.* **2013**, *12*, 5587−5597.

(10) Pinkse, M. W. H.; Uitto, P. M.; Hilhorst, M. J.; Ooms, B.; Heck, A. J. R. Selective isolation at the femtomole level of phosphopeptides from proteolytic digests using 2D-NanoLC-ESI-MS/MS and titanium oxide precolumns. *Anal. Chem.* **2004**, *76*, 3935−3943.

(11) Sweet, S. M. M.; Bailey, C. M.; Cunningham, D. L.; Heath, J. K.; Cooper, H. J. Large scale localization of protein phosphorylation by use of electron capture dissociation mass spectrometry. *Mol. Cell. Proteomics* **2009**, *8*, 904−912.

(12) Cox, J.; Mann, M. MaxQuant enables high peptide identification rates, individualized p.p.b.-range mass accuracies and proteome-wide protein quantification. *Nat. Biotechnol.* **2008**, *26*, 1367−1372.

(13) Guevremont, R. High-field asymmetric waveform ion mobility spectrometry: A new tool for mass spectrometry. *J. Chromatogr. A* **2004**, *1058*, 3−19.

(14) Saba, J.; Bonneil, E.; Pomies, C.; Eng, K.; Thibault, P. Enhanced Sensitivity in Proteomics Experiments Using FAIMS Coupled with a Hybrid Linear Ion Trap/Orbitrap Mass Spectrometer. *J. Proteome Res.* **2009**, *8*, 3355−3366.

(15) Swearingen, K. E.; Hoopmann, M. R.; Johnson, R. S.; Saleem, R. a.; Aitchison, J. D.; Moritz, R. L. Nanospray FAIMS Fractionation Provides Significant Increases in Proteome Coverage of Unfractionated Complex Protein Digests. *Mol. Cell. Proteomics* **2012**, *11*, M111.014985.

(16) Creese, A. J.; Smart, J.; Cooper, H. J. Large-scale analysis of peptide sequence variants: the case for high-field asymmetric waveform ion mobility spectrometry. *Anal. Chem.* **2013**, *85*, 4836−4843.

(17) Bridon, G.; Bonneil, E.; Muratore-Schroeder, T.; Caron-Lizotte, O.; Thibault, P. Improvement of phosphoproteome analyses using FAIMS and decision tree fragmentation. application to the insulin signaling pathway in Drosophila melanogaster S2 cells. *J. Proteome Res.* **2012**, *11*, 927−940.

(18) Creese, A. J.; Shimwell, N. J.; Larkins, K. P. B.; Heath, J. K.; Cooper, H. J. Probing the complementarity of FAIMS and strong cation exchange chromatography in shotgun proteomics. *J. Am. Soc. Mass Spectrom.* **2013**, *24*, 431−443.

(19) Xia, Y.-Q.; Wu, S. T.; Jemal, M. LC-FAIMS-MS/MS for quantification of a peptide in plasma and evaluation of FAIMS global selectivity from plasma components. *Anal. Chem.* **2008**, *80*, 7137−7143.

(20) Cunningham, D. L.; Sweet, S. M. M.; Cooper, H. J.; Heath, J. K. *Differential Phosphoproteomics of Fibroblast Growth Factor Signaling: Identification of Src Family Kinase-Mediated Phosphorylation Events research articles* **2010**, *9*, 2317−2328.

(21) Ong, S.-E.; Blagoev, B.; Kratchmarova, I.; Kristensen, D. B.; Steen, H.; Pandey, A.; Mann, M. Stable isotope labeling by amino acids in cell culture, SILAC, as a simple and accurate approach to expression proteomics. *Mol. Cell. Proteomics* **2002**, *1*, 376−386.

(22) Mohammadi, M. Structures of the Tyrosine Kinase Domain of Fibroblast Growth Factor Receptor in Complex with Inhibitors. *Science (Washington, DC, U. S.)* **1997**, *276*, 955−960.

(23) Das, J.; Chen, P.; Norris, D.; Padmanabha, R.; Lin, J.; Moquin, R. V.; Shen, Z.; Cook, L. S.; Doweyko, A. M.; Pitt, S.; et al. 2-aminothiazole

as a novel kinase inhibitor template. Structure-activity relationship studies toward the discovery of N-(2-chloro-6-methylphenyl)-2-[[6-[4-(2-hydroxyethyl)-1- piperazinyl]]-2-methyl-4-pyrimidinyl]amino)]-1,3-thiazole-5-carboxamide (Dasatinib, BMS-354825) as a Potent pan-Src Kinase Inhibitor. *J. Med. Chem.* **2006**, *49*, 6819−6832.

(24) Zhao, X.; Wang, Q.; Wang, S.; Zou, X.; An, M.; Zhang, X.; Ji, J. Citric acid-assisted two-step enrichment with TiO2 enhances the separation of multi- and monophosphorylated peptides and increases phosphoprotein profiling. *J. Proteome Res.* **2013**, *12*, 2467−2476.

(25) Olsen, J. V.; Blagoev, B.; Gnad, F.; Macek, B.; Kumar, C.; Mortensen, P.; Mann, M. Global, in vivo, and site-specific phosphorylation dynamics in signaling networks. *Cell* **2006**, *127*, 635−648.

(26) Helling, S.; Shinde, S.; Brosseron, F.; Schnabel, A.; Müller, T.; Meyer, H. E.; Marcus, K.; Sellergren, B. Ultratrace enrichment of tyrosine phosphorylated peptides on an imprinted polymer. *Anal. Chem.* **2011**, *83*, 1862−1865.

(27) Edelmann, M. J. Strong cation exchange chromatography in analysis of posttranslational modifications: innovations and perspectives. *J. Biomed. Biotechnol.* **2011**, *2011*, 936508.

(28) Barnett, D. a; Ding, L.; Ells, B.; Purves, R. W.; Guevremont, R. Tandem mass spectra of tryptic peptides at signal-to-background ratios approaching unity using electrospray ionization high-field asymmetric waveform ion mobility spectrometry/hybrid quadrupole time-of-flight mass spectrometry. *Rapid Commun. Mass Spectrom.* **2002**, *16*, 676−680.

(29) Hornbeck, P. V.; Kornhauser, J. M.; Tkachev, S.; Zhang, B.; Skrzypek, E.; Murray, B.; Latham, V.; Sullivan, M. PhosphoSitePlus: a comprehensive resource for investigating the structure and function of experimentally determined post-translational modifications in man and mouse. *Nucleic Acids Res.* **2012**, *40*, D261−D270.

(30) Chou, M. F.; Schwartz, D. Using the scan-x Web site to predict protein post-translational modifications. *Curr. Protoc. Bioinformatics* **2011**, DOI: 10.1002/0471250953.bi1316s36.

(31) Mansour, S. J.; Matten, W. T.; Hermann, A. S.; Candia, J. M.; Rong, S.; Fukasawa, K.; Vande Woude, G. F.; Ahn, N. G. Transformation of mammalian cells by constitutively active MAP kinase kinase. *Science* **1994**, *265*, 966−970.

(32) Huang, D. W.; Sherman, B. T.; Lempicki, R. A. Systematic and integrative analysis of large gene lists using DAVID bioinformatics resources. *Nat. Protoc.* **2008**, *4*, 44−57.

(33) Hashiguchi, M.; Kobori, H.; Ritprajak, P.; Kamimura, Y.; Kozono, H.; Azuma, M. Triggering receptor expressed on myeloid cell-like transcript 2 (TLT-2) is a counter-receptor for B7-H3 and enhances T cell responses. *Proc. Natl. Acad. Sci. U. S. A.* **2008**, *105*, 10495−10500.

(34) Roy, R.; Durie, D.; Li, H.; Liu, B.-Q.; Skehel, J. M.; Mauri, F.; Cuorvo, L. V.; Barbareschi, M.; Guo, L.; Holcik, M.; et al. hnRNPA1 couples nuclear export and translation of specific mRNAs downstream of FGF-2/S6K2 signalling. *Nucleic Acids Res.* **2014**, *42*, 12483−12497.

(35) van Agthoven, T.; van Agthoven, T. L. A.; Dekker, A.; van der Spek, P. J.; Vreede, L.; Dorssers, L. C. Identification of BCAR3 by a random search for genes involved in antiestrogen resistance of human breast cancer cells. *EMBO J.* **1998**, *17*, 2799−2808.

(36) Makkinje, A.; Vanden Borre, P.; Near, R. I.; Patel, P. S.; Lerner, A. Breast cancer anti-estrogen resistance 3 (BCAR3) protein augments binding of the c-Src SH3 domain to Crk-associated substrate (p130cas). *J. Biol. Chem.* **2012**, *287*, 27703−27714.

(37) Varedi, S. M.; Ventura, A. C.; Merajver, S. D.; Lin, X. N. Multisite phosphorylation provides an effective and flexible mechanism for switch-like protein degradation. *PLoS One* **2010**, *5*, e14029.

(38) Valk, E.; Venta, R.; Ord, M.; Faustova, I.; Kõivomägi, M.; Loog, M. Multistep phosphorylation systems: tunable components of biological signaling circuits. *Mol. Biol. Cell* **2014**, *25*, 3456−3460.

(39) Gunawardena, J. Distributivity and processivity in multisite phosphorylation can be distinguished through steady-state invariants. *Biophys. J.* **2007**, *93*, 3828−3834.

(40) Jin, J.; Pawson, T. Modular evolution of phosphorylation-based signalling systems. *Philos. Trans. R. Soc., B* **2012**, *367*, 2540−2555.

(41) Lee, J. Y.; Chiu, Y.-H.; Asara, J.; Cantley, L. C. Inhibition of PI3K binding to activators by serine phosphorylation of PI3K regulatory

subunit p85alpha Src homology-2 domains. *Proc. Natl. Acad. Sci. U. S. A.* **2011**, *108*, 14157−14162.